

## Supporting Information

### **Interfacial Covalent Bonding Coupled Ultrafine CuS-nanocrystals/MXene Heterostructure for Efficient and Durable Magnesium Storage**

Zhi Cheng<sup>a, b</sup>, Yanan Xu<sup>a, c, \*</sup>, Xudong Zhang<sup>a, c</sup>, Qifan Peng<sup>a, c</sup>, Kai Wang<sup>a, c</sup>, Xiong Zhang<sup>a, c</sup>, Xianzhong Sun<sup>a, c</sup>, Qinyou An<sup>b, \*</sup>, Liqiang Mai<sup>b</sup> and Yanwei Ma<sup>a, c, d, \*</sup>

a. Institute of Electrical Engineering, Chinese Academy of Sciences, Beijing 100190, China

b. State Key Laboratory of Advanced Technology for Materials Synthesis and Processing, Wuhan University of Technology, Hubei, Wuhan 430070, China.

c. School of Engineering Sciences, University of Chinese Academy of Sciences, Beijing 100049, China

d. School of Materials Science and Engineering, Zhengzhou University, Zhengzhou, Henan 450001, China

\*Corresponding author:

E-mail: xuyanan@mail.iee.ac.cn; anqinyou86@whut.edu.cn; ywma@mail.iee.ac.cn

## 1 Experimental Section

### 1.1 Delamination of $\text{Ti}_3\text{C}_2\text{T}_x$ MXene

The multilayer  $\text{Ti}_3\text{C}_2\text{T}_x$  powder (m- $\text{Ti}_3\text{C}_2\text{T}_x$ ) was obtained after etching  $\text{Ti}_3\text{AlC}_2$  MAX phase with hydrofluoric acid (HF). Then m- $\text{Ti}_3\text{C}_2\text{T}_x$  (200 mg) was dispersed in tetrabutylammonium hydroxide solution (TBAOH~25% in  $\text{H}_2\text{O}$ , 7mL) and stirred for 18 hours at 35 °C and the suspension was centrifugated at 8000 r/min for 5 minutes to obtain the precipitant. Then, the product was put into 30 mL deionized water and sonicated for 2 hours with ice bath. Finally, the delaminated  $\text{Ti}_3\text{C}_2\text{T}_x$  (d-  $\text{Ti}_3\text{C}_2\text{T}_x$ ) suspension was collected from supernatant after centrifugation at 4000 r/min for 20 minutes.

### 1.2 Synthesis of CuS nanoparticles and CuS/d- $\text{Ti}_3\text{C}_2\text{T}_x$ composite

The CuS sample was synthesized by a typical hydrothermal method. Copper chloride dihydrate (1 mmol, 0.1023 g,  $\text{CuCl}_2 \cdot 2\text{H}_2\text{O}$ ) and L-cysteine (0.1745 g,  $\text{HOOCCH}(\text{NH}_2)\text{CH}_2\text{SH}$ ) were dissolved into deionized water. Then, the solution was transferred into 50 mL Teflon-lined stain-steel autoclave and heated for 8h at 160 °C before cooling to room temperature. Finally, the black precipitation was separated by centrifugation, washed several times with deionized water and ethanol and dried overnight in a vacuum oven at 70 °C, to obtain the as-synthesized CuS sample.

For synthesis of CuS/d- $\text{Ti}_3\text{C}_2\text{T}_x$ , d- $\text{Ti}_3\text{C}_2\text{T}_x$  suspension ( $\sim 10 \text{ mg mL}^{-1}$ , 2.5 mL) was added to the solution of cupric chloride dihydrate (1 mmol, 0.1023 g,  $\text{CuCl}_2 \cdot 2\text{H}_2\text{O}$ ) and L-cysteine (0.1745 g,  $\text{HOOCCH}(\text{NH}_2)\text{CH}_2\text{SH}$ ) before transferred into 50 mL Teflon-lined stain-steel autoclave. The subsequent experimental procedure including heat-treatment and collection of CuS/d-  $\text{Ti}_3\text{C}_2\text{T}_x$  sample was the same as that of CuS sample described above. The mass proportion of CuS nanoparticles in CuS/d- $\text{Ti}_3\text{C}_2\text{T}_x$  is about 79wt%.

### 1.3 Materials characterizations

The crystal structures of the products were characterized by a multifunctional Bruker D8 X-ray diffractometer with Cu K $\alpha$  radiation ( $\lambda=1.54060$  Å). Raman spectra were measured on LabRam HR-800, Horiba Jobin Yvon with excitation wavelength of 532 nm. The X-ray photoelectron spectra (XPS) of the samples were conducted on Nexsa to investigate the chemical states. The morphology and elemental compositions of the samples were characterized by SEM (ZEISS SIGMA) equipped with EDS. TEM images were recorded by using a JEM-F200 microscope.

### 1.4 Electrochemical measurements:

The electrochemical properties were characterized by assembling 2032 coin-type battery cells in an Ar-filled glove box ( $O_2 \leq 1$  ppm and  $H_2O \leq 1$  ppm). The cathodic working electrodes were fabricated by mixing CuS or CuS/d-Ti $_3$ C $_2$ T $_x$  with super C45 and poly tetra fluoroethylene (PTFE) binder at a ratio of 7:2:1. The active material loading of was about 3.0-3.5 mg cm $^{-2}$ , and ultra-thin molybdenum foil was selected as the current collector. With all phenyl complex/tetrahydrofuran (APC, 41.2% 2M MgPhCl/THF, 5.3% AlCl $_3$ , 53.4% THF) as electrolyte, magnesium foils were employed as anode. The galvanostatic charge-discharge (GCD) tests and galvanostatic intermittent titration technique (GITT) tests were performed on LAND battery tester within the potential range of 0.1-2.0 V. Cyclic voltammetry (CV) curves were acquired through a BioLogic VMP3 electrochemical analyzer.

### 1.5 Computational method

We have employed the Vienna Ab initio Simulation Package (VASP) to perform all density functional theory (DFT) calculations within the generalized gradient approximation (GGA) using the Perdew-Burke-Ernzerhof (PBE) functional. Spin-polarization effect was also considered.<sup>1, 2</sup> We have chosen the projected augmented wave (PAW) potentials to describe the ionic cores and take valence electrons into

account using a plane wave basis set with a kinetic energy cutoff of 400 eV. Geometry optimizations were performed with the force convergency smaller than 0.05 eV/Å. The DFT-D3 empirical correction method was employed to describe van der Waals interactions. Monkhorst-Pack k-points of  $1 \times 1 \times 1$  was applied for all the calculations. All atoms are relaxed in d-Ti<sub>3</sub>C<sub>2</sub>T<sub>x</sub> MXene and CuS/d-Ti<sub>3</sub>C<sub>2</sub>T<sub>x</sub>. Half atoms at bottom are fixed in the CuS (002). The adsorption energy ( $E_a$ ) is calculated by the equation:  $E_a = E(\text{total}) - E(\text{slab}) - E(\text{reference})$ , where  $E(\text{total})$  and  $E(\text{slab})$  are the total energy of the surface slab with and without adsorption, respectively, and  $E(\text{reference})$  is the energy of the Mg and MgS bulk.

## 2 Figures and Tables

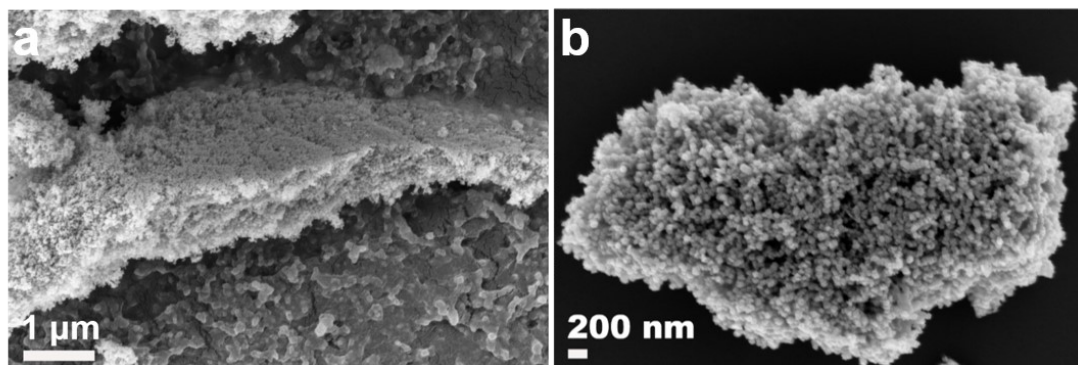


**Fig. S1** (a) Low-magnification and (b) high-magnification SEM images of CuS nanoparticles.

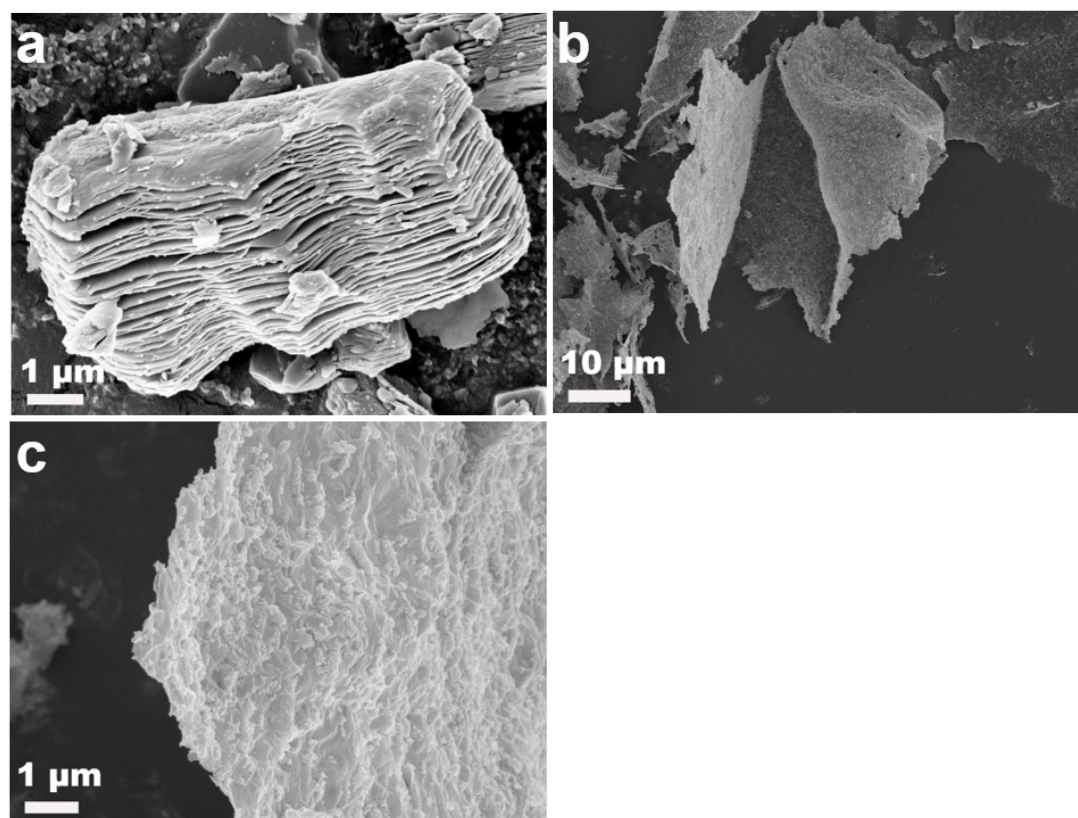


**Fig. S2** (a) Accordion-like m-Ti<sub>3</sub>C<sub>2</sub>T<sub>x</sub> SEM image. (b) Low magnification and (c) high magnification SEM images of d-Ti<sub>3</sub>C<sub>2</sub>T<sub>x</sub> nanoflakes.

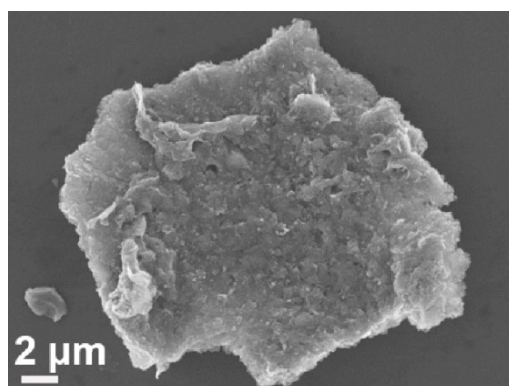


Fig. S3 SEM image of CuS/d-Ti<sub>3</sub>C<sub>2</sub>T<sub>x</sub> corresponding to the EDS mapping images.

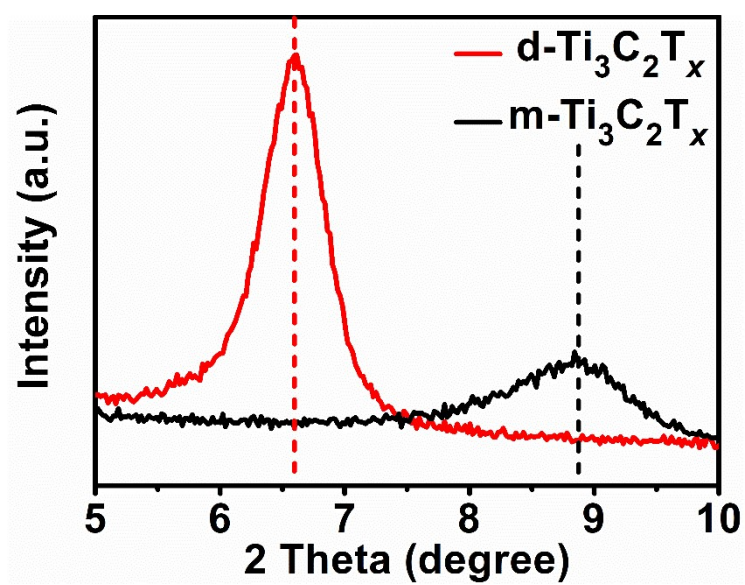


Fig. S4 XRD pattern of accordion-like m-Ti<sub>3</sub>C<sub>2</sub>T<sub>x</sub> and d-Ti<sub>3</sub>C<sub>2</sub>T<sub>x</sub> nanoflakes.

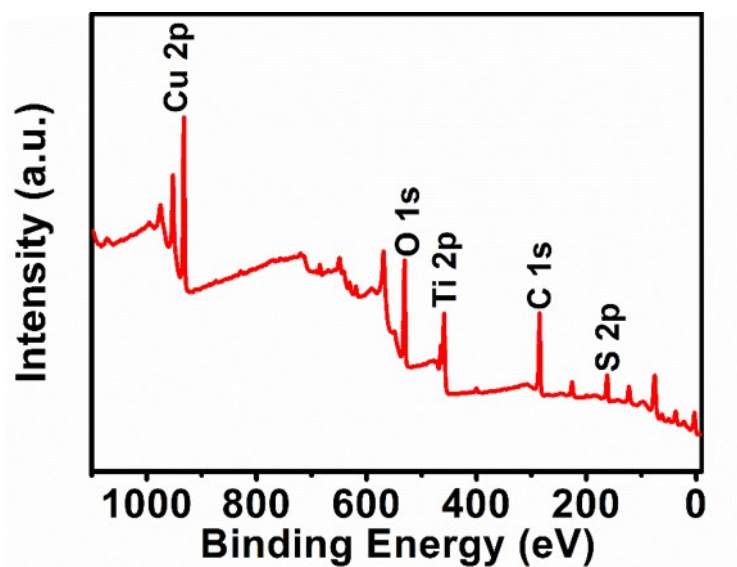


Fig. S5 XPS full survey spectrum of CuS/d-Ti<sub>3</sub>C<sub>2</sub>T<sub>x</sub>.

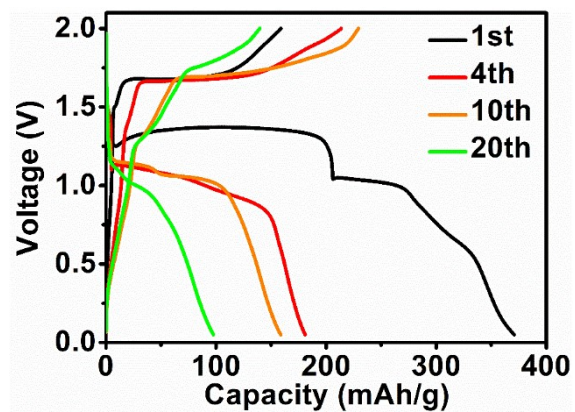
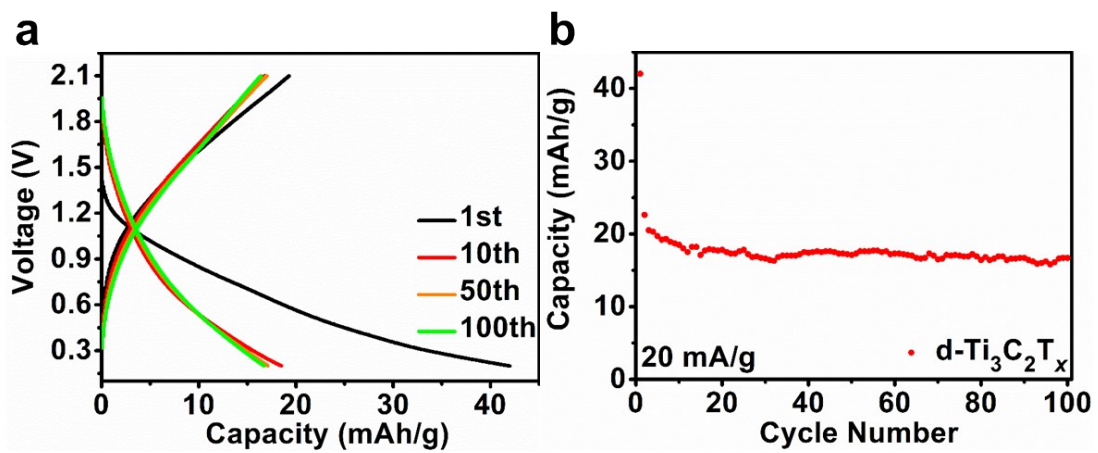
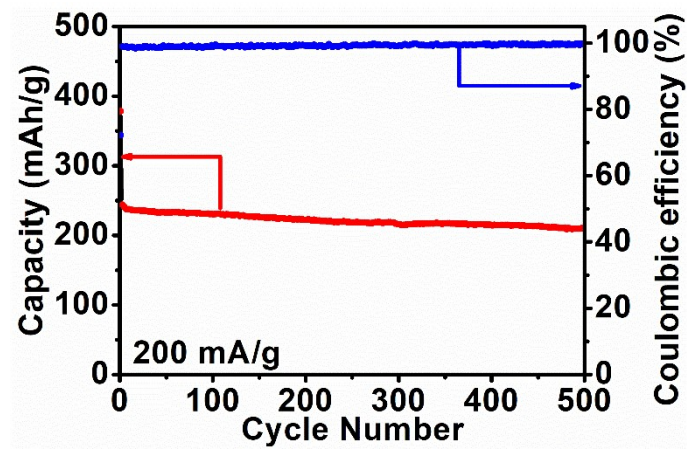


Fig. S6 Discharge/charge curves of pure CuS cathode at 50 mA g<sup>-1</sup> in different cycles.



**Fig. S7** (a) Discharge/charge curves and (b) cycling performance of d-Ti<sub>3</sub>C<sub>2</sub>T<sub>x</sub> cathode at current density of 20 mA g<sup>-1</sup>.



**Fig. S8.** Cycling performance of CuS/d-Ti<sub>3</sub>C<sub>2</sub>T<sub>x</sub> cathode at current density of 200 mA g<sup>-1</sup>.

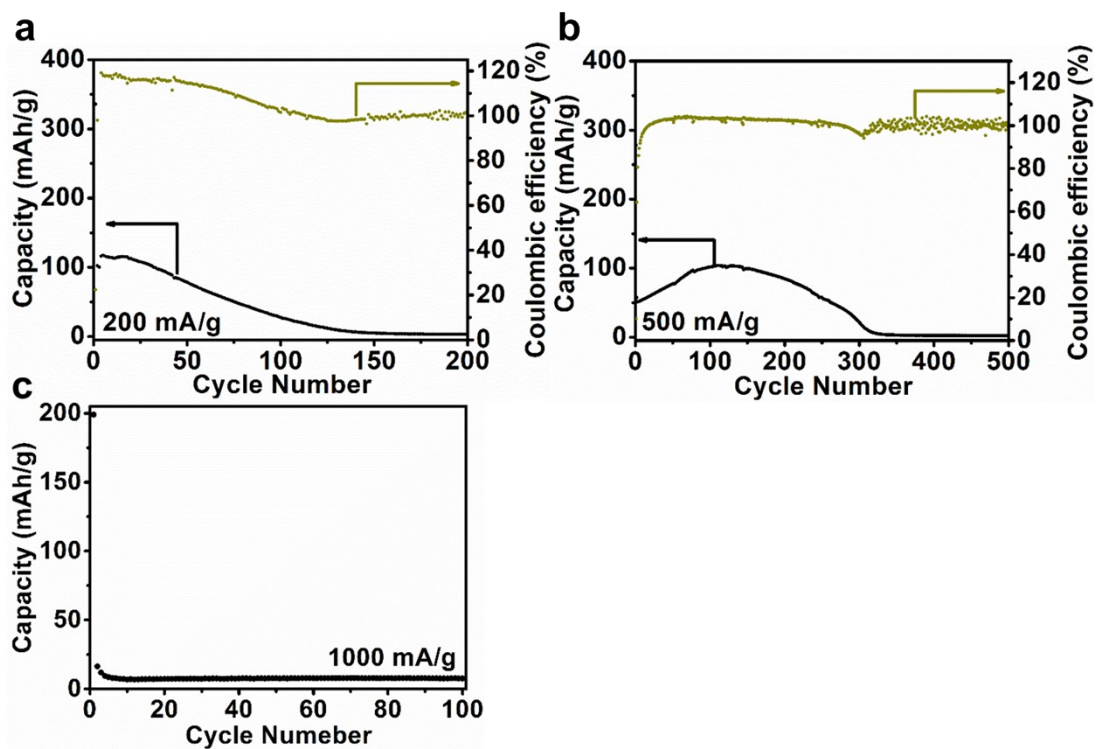


**Fig. S9** Cycling performance of pure CuS cathode at current densities of (a) 200 mA g<sup>-1</sup> (b) 500 mA g<sup>-1</sup> and (c) 1000 mA g<sup>-1</sup>.

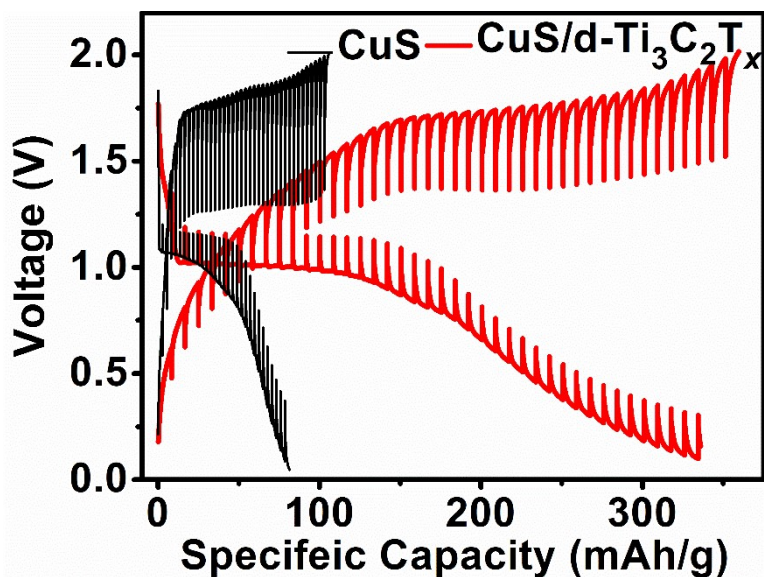


**Fig. S10** GITT curves of CuS and CuS/d-Ti<sub>3</sub>C<sub>2</sub>T<sub>x</sub> cathodes at a constant current pulse of 20 mA for 5 min followed by a rest time of 10 min.

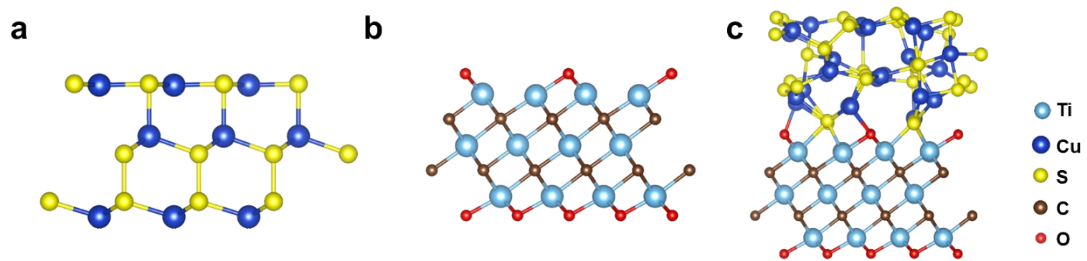


**Fig. S11** The clean chemical structure models of (a) CuS, (b) d-Ti<sub>3</sub>C<sub>2</sub>T<sub>x</sub> MXene and (c) CuS/d-Ti<sub>3</sub>C<sub>2</sub>T<sub>x</sub>.

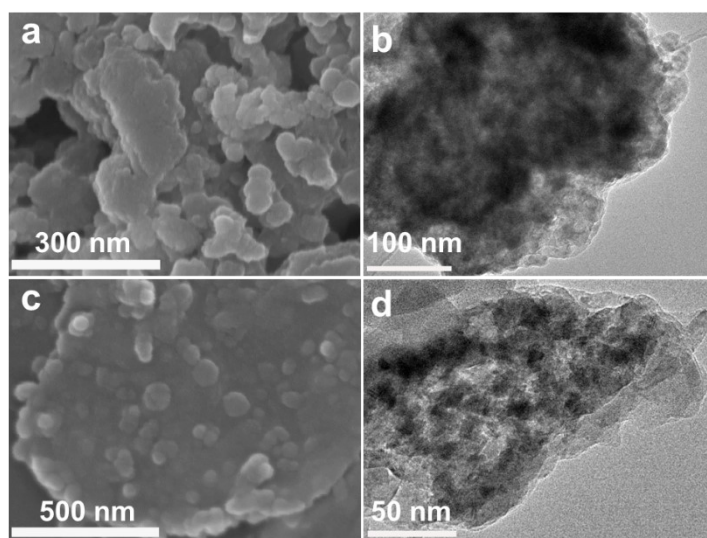


**Fig. S12.** The SEM and TEM images of (a, b) CuS and (c, d) CuS/d-Ti<sub>3</sub>C<sub>2</sub>T<sub>x</sub> electrodes after 50 cycles at 50 mA g<sup>-1</sup>.

**Table S1.** Summary of long cycling performance of CuS cathode materials for RMBs.

Cathode materials	Discharge capacity/ (mAh·g <sup>-1</sup> )	Operating voltage/V	Mass loading/ (mg cm <sup>-2</sup> )	Cycling performance/ (mAh·g <sup>-1</sup> )/Cycles	Rate performance/ (mAh·g <sup>-1</sup> )	Refs.
CuS nanospheres	361 at 50 mA·g <sup>-1</sup>	0.8-2.4	5-7	153/20 (50 mA·g <sup>-1</sup> )	-	3
CuS nanoparticles	175 at 50 mA·g <sup>-1</sup>	0.3-2.2	~3.5	120/350 (50 mA·g <sup>-1</sup> )	90 at 1000 mA·g <sup>-1</sup>	4
CuS nanosheets	300 at 20 mA·g <sup>-1</sup>	0-2.0	1.0-1.5	135/200 (200 mA·g <sup>-1</sup> )	237.5 at 100 mA·g <sup>-1</sup>	5
CuS nanoparticles	300 at 100 mA·g <sup>-1</sup>	0-2.3	-	290/200 (100 mA·g <sup>-1</sup> )	-	6
CuS microspheres	430 at 5 mA·g <sup>-1</sup>	0.5-2.2	-	400/80 (5 mA·g <sup>-1</sup> )	-	7
CuS nanocubes	200 at 100 mA·g <sup>-1</sup>	0.05-2.5	1.5	50/200 (1000 mA·g <sup>-1</sup> )	50 at 1000 mA·g <sup>-1</sup>	8
CuS nanocages	370 at 50 mA·g <sup>-1</sup>	0.2-2.0	3.5-5	167/40 (100 mA·g <sup>-1</sup> )	-	9
CuS nanotubes	281.2 at 20 mA·g <sup>-1</sup>	0.1-2.1	1.5-2.0	58.1/550 (1000 mA·g <sup>-1</sup> )	140 at 200 mA·g <sup>-1</sup>	10
CuS microspheres	252 at 100 mA·g <sup>-1</sup>	0.1-2.1	1.0-2.0	60/500 (1000 mA·g <sup>-1</sup> )	160 at 200 mA·g <sup>-1</sup>	11
CuS@rGO	421 at 50 mA·g <sup>-1</sup>	0.1-2.1	1.5	50.9/500 (1000 mA·g <sup>-1</sup> )	193 at 500 mA·g <sup>-1</sup>	12
CuS/d-Ti <sub>3</sub> C <sub>2</sub> T <sub>x</sub>	336.5 at 50 mA·g <sup>-1</sup>	0.1-2.0	3.0-3.5	92.2/1000 (1000 mA·g <sup>-1</sup> )	117.1 at 1000 mA·g <sup>-1</sup>	This work

## References

- 1 W. Kohn and L. J. Sham, *Physical Review*, 1965, **140**, A1133-A1138.
- 2 J. D. Pack and H. J. Monkhorst, *Physical Review B*, 1977, **16**, 1748-1749.
- 3 F. Xiong, Y. Fan, S. Tan, L. Zhou, Y. Xu, C. Pei, Q. An and L. Mai, *Nano Energy*, 2018, **47**, 210-216.
- 4 M. Wu, Y. Zhang, T. Li, Z. Chen, S. Cao and F. Xu, *NANOSCALE*, 2018, **10**, 12526-12534.
- 5 Z. Wang, S. Rafai, C. Qiao, J. Jia, Y. Zhu, X. Ma and C. Cao, *ACS Appl. Mater. Interfaces*, 2019, **11**, 7046-7054.
- 6 K. V. Kravchyk, R. Widmer, R. Erni, R. J. C. Dubey, F. Krumeich, M. V. Kovalenko and M. I. Bodnarchuk, *Sci. Rep.*, 2019, **9**, 7988.
- 7 M. Mao, T. Gao, S. Hou, F. Wang, J. Chen, Z. Wei, X. Fan, X. Ji, J. Ma and C. Wang, *Nano Lett.*, 2019, **19**, 6665-6672.
- 8 J. Shen, Y. Zhang, D. Chen, X. Li, Z. Chen, S. Cao, T. Li and F. Xu, *J. Mater. Chem. A*, 2019, **7**, 21410-21420.
- 9 W. Ren, F. Xiong, Y. Fan, Y. Xiong and Z. Jian, *ACS Appl. Mater. Interfaces*, 2020, **12**, 10471-10478.
- 10 C. Du, Y. Zhu, Z. Wang, L. Wang, W. Younas, X. Ma and C. Cao, *ACS Appl. Mater. Interfaces*, 2020, **12**, 35035-35042.
- 11 J. Huang, Y. Zhu, C. Du, Z. Han, X. Yao, X. Yang, Y. Cao, Y. Zhang, X. Ma and C. Cao, *Electrochim. Acta*, 2021, **388**, 138619.

12 Z. Wang, Y. Zhang, H. Peng, C. Du, Z. Han, X. Ma, Y. Zhu and C. Cao, *Electrochim. Acta*, 2022, **407**, 139786.